van der Waals Interactions between Nanotubes and Nanoparticles for Controlled Assembly of Composite Nanostructures

Graham A. Rance, Dan H. Marsh, Stephen J. Bourne, Thomas J. Reade, and Andrei N. Khlobystov*

School of Chemistry, University of Nottingham, University Park, Nottingham NG7 2RD, United Kingdom

ABSTRACT We have demonstrated that ubiquitous van der Waals forces are significant in controlling the interactions between nanoparticles and nanotubes. The adsorption of gold nanoparticles (AuNPs) on nanotubes (MWNTs) obeys a simple quadratic dependence on the nanotube surface area, regardless of the source of AuNPs and MWNTs. Changes in the geometric parameters of the components have pronounced effects on the affinity of nanoparticles for nanotubes, with larger, more polarizable nanostructures exhibiting stronger attractive interactions, the impact of which changes in the following order MWNT diameter > AuNP diameter > MWNT length.

Deposition of nanoparticles on quasi-1D structures with one macroscopic and two nanoscopic dimensions is one of the most efficient ways of harnessing their fascinating size-dependent properties.[1−6] Recently nanotube−nanoparticle composites have opened significant new avenues for novel applications, specifically those technologies involved in catalysis,[7,8] chemical sensing,[9,10] microelectronics,[11] neural nets,[12] and photovoltaics.[13] There is, however, a critical lack of understanding concerning the nature, strength, and reversibility of the interactions that exist between nanoparticles and nanotubes. This limited knowledge hinders the ability to design and manipulate the assembled nanocomposite materials in a controlled, user-specified fashion.

Though DVLO theory, which assumes that the separation between particles is controlled by the balance between Coulombic and van der Waals forces,[14] is often employed to describe the total interaction potential between microscopic objects, its applicability to nanoscale entities has yet to be established. However, Coulombic interactions have been recently successfully utilized for the assembly of materials in the nanometer size regime.[15−17] This is largely due to the fact that these forces are well understood and constitute the most long-range and highest strength (nonbonding) interactions that can be envisioned between species. Moreover, both the sign and magnitude of electrostatic interactions can be discretely modulated by controlling the surface charge of nanostructures[18,19] and the properties of the medium,[20,21] respectively, and consequently nano- and mesoscopic structures of remarkable complexity have been assembled utilizing the principles of charge−charge interactions.[15−17] By contrast, van der Waals interactions are often overlooked for the controlled assembly of nanostructures as they are often perceived as too short-range and weak to be useful. A unique property of van der Waals interactions, somewhat analogous to the gravitation force, however, is that this force is *omnipresent* and *always attractive*, apart from very rare examples involving dislike materials.[22] Just like the detailed understanding of the gravitation force in the past has enabled the launching of space vehicles with remarkable precision into their orbits, the understanding of the properties of van der Waals interactions on the nanoscale has the potential to open new avenues for the assembly of materials with well-defined structure and thus functional properties.

In this study, we investigate the fundamental properties of van der Waals interactions between nanoparticles and nanotubes. We demonstrate that these interactions are significant and crucially depend on the structural parameters of the component nanostructures. For the first time, we have demonstrated that composition and structure of nanoparticle−
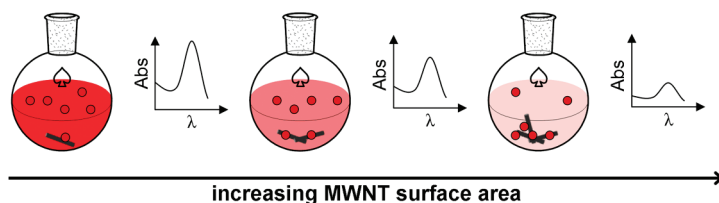
Figure 1. Schematic representation of the experimental methodology. MWNTs (of known mass/surface area) are added to a solution of AuNPs (of known concentration), the combined mixture is homogenized and allowed to equilibrate, and finally MWNTs with AuNPs adsorbed on their surface are separated from AuNPs remaining in solution.[25] The number of (unadsorbed) AuNPs remaining in solution can be quantified using UV−vis spectroscopy. The number of (adsorbed) AuNPs can be determined using TEM.

nanotube assemblies can be precisely controlled through van der Waals interactions between the nanoscale species.

RESULTS AND DISCUSSION

In our experiments, we have investigated the solution-phase interactions of free-standing, discrete nanoparticles with carbon nanotubes. Multiwalled carbon nanotubes (MWNTs) were selected for our studies because, unlike single-walled carbon nanotubes (SWNTs), which are known to bundle significantly in both solid state and solution, MWNTs typically exist as discrete nanostructures,[23] and as such, we were able to probe the interactions between nanoparticles and isolated nanotubes rather than complex, indefinable aggregates. Citrate-stabilized gold nanoparticles (AuNPs) were chosen as colloidal species of this metal exhibit a strong absorption in the visible range due to the surface plasmon resonance (SPR) absorbance. Solutions are typically colored ruby-red, and the actual color (*i.e.*, the absolute intensity of the SPR peak) is directly related to the concentration of AuNPs present. Furthermore, addition of nanotubes causes measurable changes in the color of the mixed suspension due to the sequestering of AuNPs by nanotubes.[20,24] Therefore, the number of AuNPs removed from the bulk solution and deposited on MWNTs can be conveniently quantified by UV−vis absorption spectroscopy (Figure 1).

In our measurements, both nanotubes and nanoparticles carry negative surface charges, the origins of which are associated with carboxylic acid groups formed as a result of partial oxidation of nanotube surface carbon atoms during synthesis[26] and those that comprise the nanoparticle stabilizing layer,[27] respectively. This means that AuNPs do not adsorb spontaneously and must overcome an energy barrier dictated by the charges x^- and y^- on nanotube and nanoparticle surfaces, respectively (Figure 2a). Attractive interactions in this system are therefore governed only by short-range forces. Considering the fact that the Hamaker constant, which defines the pair potential between nanoparticles and nanotubes, is large (6.0×10^{-19} J for gold nanoparticles and multiwalled carbon nanotubes)[28,29] and the po-

larizability of both components is high, these short-range attractive interactions must be associated with van der Waals forces. Furthermore, as carbon nanotubes are spatially extended one-dimensional, electrically conducting structures with plasmonic electrons, van der Waals interactions with other nanoscale and molecular species are likely to be
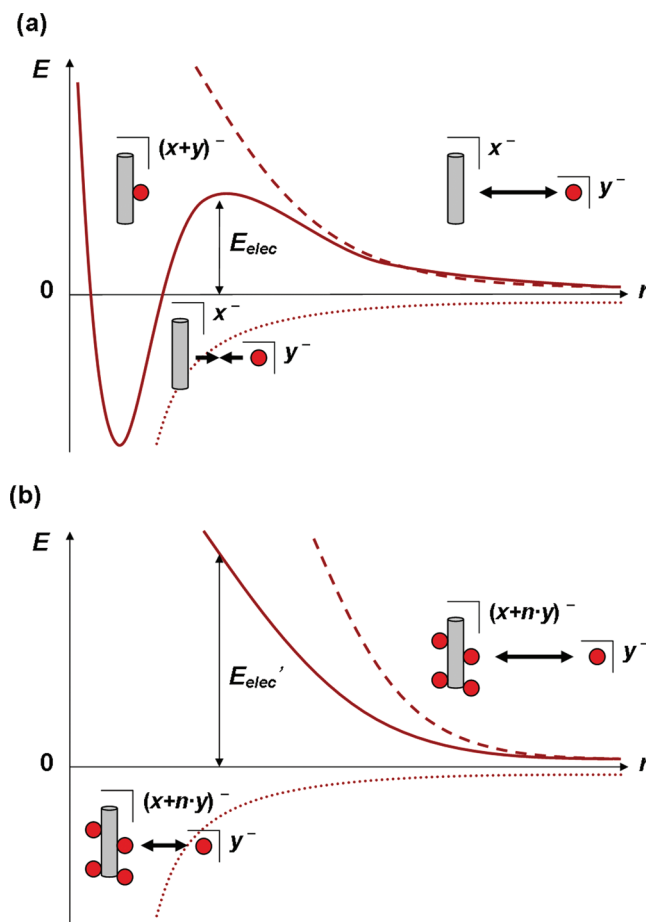

Figure 2. Schematic representation of the relative energies of the repulsive Coulombic (dashed line) and attractive van der Waals (dotted line) forces as a function of distance between negatively charged nanoparticles and negatively charged nanotubes. (a) Initially, nanoparticles have to overcome the barrier E_{elec} provided by electrostatic repulsion of x^- and y^- surface charges on MWNTs and AuNPs, respectively. (b) As more nanoparticles adsorb on nanotubes, the electrostatic repulsion increases ($E_{elec}' > E_{elec}$) eventually halting the adsorption process. The arrows reflect the sign and magnitude of the interactions between the two nanoscopic species. Surface functional groups have been omitted for clarity.

TABLE 1. Characterization of Large and Small AuNPs[a]

sample	λ/nm	ε/ dm³mol⁻¹cm⁻¹	d_{NP}/ nm	d_{NP}^*/nm	PDI	ζ/mV
large AuNP	524.1	1.5×10^9	20.6 ± 1.4	24.6	0.15	-38.5 ± 3.9
small AuNP	519.5	2.5×10^8	13.1 ± 0.9	15.6	0.15	-23.2 ± 4.8

[a]The λ and ε are the wavelength and extinction coefficient of the SPR absorbance, respectively, as determined by UV−vis spectroscopy; d_{NP} is the mean nanoparticle diameter as determined by TEM; d_{NP}^* and PDI are the mean nanoparticle diameter and polydispersity index, respectively, as determined by dynamic light scattering (DLS); ζ is the surface potential as determined by phase analysis light scattering (PALS).

much more long-range ($\sim 1/r^3$) than those typically observed between colloidal species ($\sim 1/r^6$).[30] From our measurements, we have shown that the total negative charge of the AuNP−MWNT composite ($x + ny$)⁻, where n is the number of adsorbed nanoparticles, increases with n, thus leading to an increase in the repulsive electrostatic force. After a certain threshold, value of n starts dominating both long- and short-range interactions (Figure 2b) and therefore makes further adsorption of nanoparticles from solution impossible.

By modulating the energy of van der Waals forces, the depth of the energetic minimum can be tuned (Figure 2), which offers a viable route for controlling the number of nanoparticles deposited on nanotubes. Indeed, theoretical models predict that the magnitude of van der Waals interactions between carbon nanotubes, and both nanoscale[31,32] and molecular species[33,34] depend on the dimensions of the components. Our experimental methodology allows rigorous testing of how this dependence is manifested for basic geometric parameters of nanotubes and nanoparticles, such as their width and length, and provides specific protocols for controlling composition of the hybrid nanostructures.

To investigate the effect of AuNP diameter on the interactions between AuNPs and MWNTs, two nanoparticle samples possessing different mean diameters (hereafter referred to as large and small AuNPs, respectively) were prepared according to the modified citrate reduction outlined by Slot and Geuze[35] and characterized by complementary techniques (Table 1 and S.1 in the Supporting Information).

Spectroscopic, microscopic and light scattering analyses confirm that the mean nanoparticle diameters are different between samples. Assuming van der Waals forces are significant, the affinity of MWNTs for large (more polarizable) AuNPs should be greater than small (less polarizable) AuNPs.[36] To test this premise, comparative series of titration experiments were undertaken using large and small AuNPs with MWNTs (produced by arc discharge) carrying intrinsic negative surface charge of -20.6 ± 6.5 mV. The number of gold nanoparticles adsorbed at a variety of carbon nanotube masses were recorded using UV−vis spectroscopy for both nanoparticle systems and plotted as a function of the surface area of nanotubes used (Figure 3).

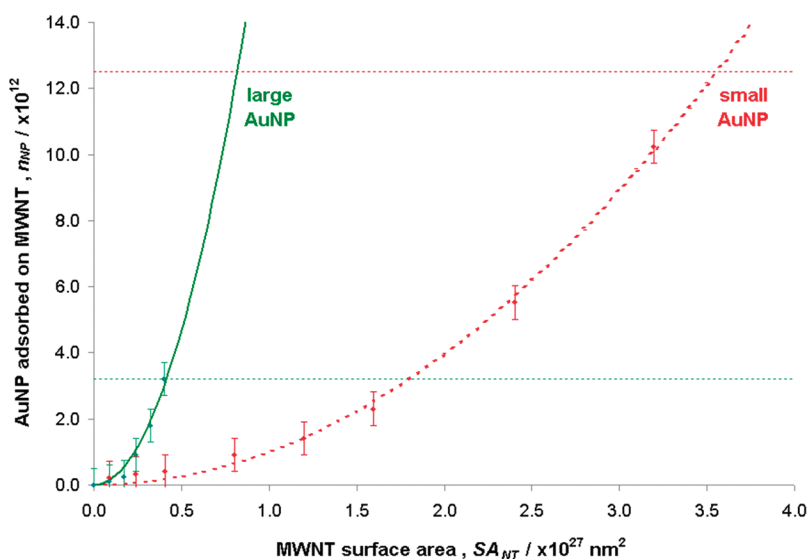There are several significant observations from analysis of this plot.

Figure 3. Adsorption isotherm correlating the number (n_{NP}) of large AuNPs (green full line, $n_{NP} = 1.87 \times 10^{-41}$ (SA$_{NT}$)², $R^2 = 0.9714$) and small AuNP (red dashed line, $n_{NP} = 9.97 \times 10^{-43}$ (SA$_{NT}$)², $R^2 = 0.9967$) independently adsorbed onto MWNTs (produced by AD) with carbon nanotube surface area (SA$_{NT}$, in nm²). The horizontal dotted line refers to the total number of nanoparticles in starting solution (3.2×10^{12} and 1.3×10^{13} for large and small AuNPs, respectively). Bars reflect the mean standard deviation from repeat measurements.
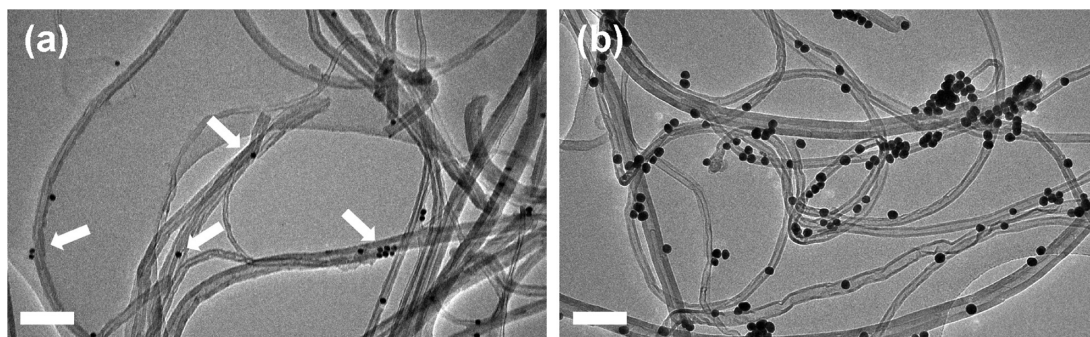
Figure 4. TEM images of (a) [small AuNP]−MWNT and (b) [large AuNP]−MWNT composite materials. The white arrows guide the eye to the precise location of some adsorbed AuNPs. Scale bars are 100 nm.

First, there is a clear smooth increase in both cases in the number of AuNPs adsorbed with increasing MWNT surface area. This is consistent with geometrical considerations, as using a larger total nanotube surface area provides a higher number of adsorption sites available for nanoparticle binding.

Second, there is a strong quadratic relationship in both cases between the number of AuNPs adsorbed and MWNT surface area ($R^2 \approx 1$). This unexpected correlation, where a disproportionately greater number of AuNPs are adsorbed at higher nanotube surface areas (S.2 in the Supporting Information), can be attributed to van der Waals interactions, the efficiency of which increases with the concentration (and thus polarizable volume) of MWNTs employed. This observation supports previous theoretical studies which looked to assess the effect of carbon nanotube morphology on the magnitude of van der Waals forces with fullerenes and other small molecules, where it was observed that the total static polarizability of nanotubes (a summation of both longitudinal and transverse components) increases in a nonlinear (quadratic) fashion with nanotube length.[33,34] Our measurements demonstrate clearly that similar rules can be applied to nanotube−nanoparticle interactions. The exact origin of this nonlinearity has yet to be fully elucidated but is likely to be the cumulative effect of anisotropy on polarizability (determined by the number of loosely bound electrons, the volume over which these electrons are spread and the extent of possible perturbation of the electron cloud).[34] Assuming that the increase of the concentration of nanotubes in aqueous suspension effectively increases the total volume accessible for delocalized electrons (higher concentration of nanotubes increases the probability of nanotube−nanotube contacts, which increase the dimensionality of the system), the behavior we experimentally observe (cooperative nanotube polarization) is analogous to that seen from theoretical considerations. Screening of charge at high concentration is an additional mechanism that may also contribute to this effect.

Finally and most importantly, the effect of AuNP diameter is unambiguously evident, with significant disparities in the MWNT surface area required to adsorb an identical number of AuNPs from solution. Clearly, the affinity toward adsorption on nanotubes is greater for larger nanoparticles, epitomized by the higher value of the prequadratic coefficient in the relationship between n_{NP} and SA_{NT} (1.87×10^{-41} and 9.97×10^{-43} for large and small AuNPs, respectively). This is in excellent qualitative agreement with previous theoretical models proposed.[31,32] Furthermore, our observations show that the enhancement of van der Waals forces for larger nanoparticles, which also carry a higher surface charge (Table 1), effectively overrides the increase in electrostatic repulsion between these AuNPs and MWNTs.

Careful microscopic analysis permits direct assessment of the precise structure of the resultant hybrid materials. Consequently, AuNP−MWNT heterostructures, prepared using identical quantities of MWNTs (mass = 0.50 mg, surface area = 4.0×10^{26} nm^2), were analyzed by TEM (Figure 4).

Microscopy confirms that all AuNPs sequestered from solution are associated with MWNTs, as virtually no free-standing AuNPs were observed in micrographs of both samples. This verifies that the observed decrease in AuNP concentration measured by spectroscopy (Figure 3) is related solely to the deposition of nanoparticles on the nanotube surface. Furthermore, the effect of AuNP diameter is instantly evident, with a significantly higher coverage of large AuNPs on MWNTs than their smaller analogues (Figure 4). To quantify this observation, statistical analysis of the number of nanoparticles adsorbed per unit carbon nanotube length (and thus

TABLE 2. Characterization of Long and Short MWNTs[a]

sample	l_{NT}/μm	id_{NT}/nm	od_{NT}/nm	W_{NT}/nm	ζ/mV
long MWNT	2.0 ± 0.3	4.4 ± 1.6	9.2 ± 2.2	10 ± 2	−11.4 ± 5.9
short MWNT	1.7 ± 0.4	4.4 ± 1.6	9.2 ± 2.2	10 ± 2	−12.9 ± 4.0

[a]The l_{NT}, id_{NT}, od_{NT}, and W_{NT} are the mean nanotube length, inner diameter, outer diameter, and number of walls, respectively, as determined by TEM.
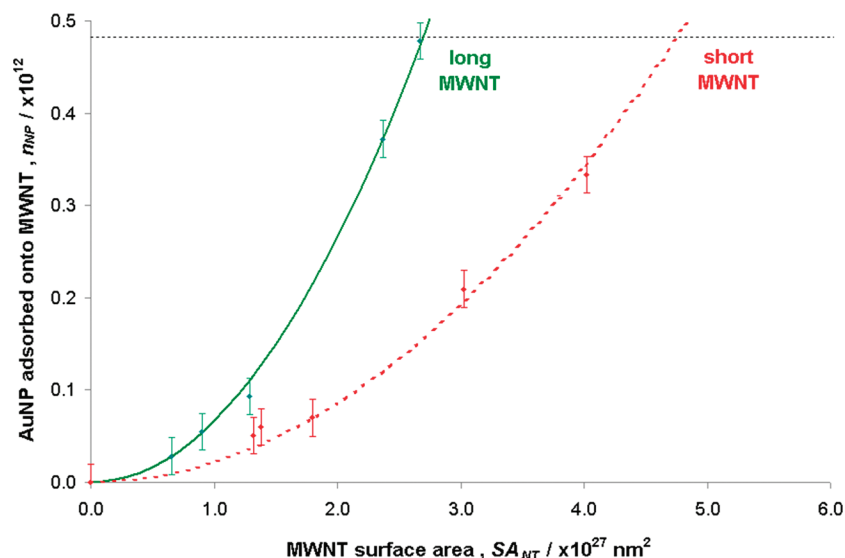
Figure 5. Adsorption isotherm correlating the number of AuNPs (n_{NP}) independently adsorbed onto long MWNTs (green full line, $n_{NP} = 6.64 \times 10^{-44} (SA_{NT})^2$, $R^2 = 0.9981$) and short MWNTs (red dashed line, $n_{NP} = 2.13 \times 10^{-44} (SA_{NT})^2$, $R^2 = 0.9852$) with carbon nanotube surface area (SA_{NT}, in nm^2). The horizontal dotted line refers to the total number of nanoparticles in starting solution (4.8×10^{11}). Bars reflect the mean standard deviation from repeat measurements.

surface area) was performed, and this was found to be 15.8 ± 1.5 μm^{-1} (1.7×10^{-4} nm^{-2}) and 1.5 ± 1.4 μm^{-1} (1.6×10^{-5} nm^{-2}) for large and small AuNPs, respectively.[37] This corresponds to an 11-fold difference in the density of adsorbed AuNPs between samples. By comparison, an 8-fold difference in the number of AuNPs sequestered from solution (3.2×10^{12} and 4.1×10^{11} for large and small AuNPs, respectively) was recorded using our spectroscopic approach. This remarkable correlation of quantitative results obtained from independent bulk and local-probe characterization methods confirms the accuracy and reproducibility of the protocol developed during this study.

From our spectroscopic and microscopic observations, we can therefore conclude that the nature of the short-range attractive interactions that result in the adsorption of nanoparticles on nanotubes (in systems with same sign surface charges) are associated with van der Waals forces as large (more polarizable) AuNPs have a greater affinity toward adsorption on MWNTs than small (less polarizable) AuNPs.

To investigate the effect of MWNT length on the interactions between AuNPs and MWNTs, two nanotube samples possessing different mean lengths (hereafter referred to as long and short MWNTs, respectively) were prepared using a conventional thermal oxidation procedure[23] and characterized (Table 2 and S.3 in the Supporting Information).

Quantitative microscopic analysis confirms that the mean nanotube lengths are different, while all other structural characteristics (specifically diameter and number of concentric tubes) remain unaffected by the shortening procedure. Assuming van der Waals forces are significant, the affinity of AuNPs for long (more polarizable) MWNTs should be greater than short (less polarizable) MWNTs. To test this concept, comparative series of titration experiments were undertaken using AuNPs (produced by the classic citrate reduction as outlined by Turkevitch et al.[38]) possessing intrinsic surface charge of -48.4 ± 5.1 mV (Figure 5).

By analogy with the titration experiments discussed in the previous section, the nonlinear rela-
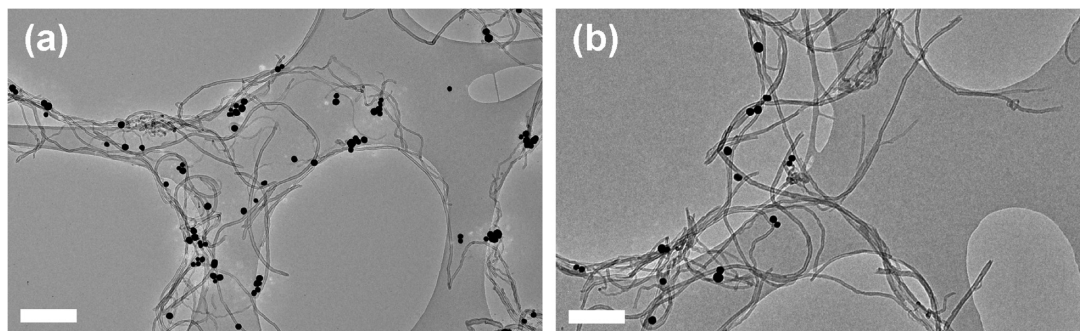

Figure 6. TEM imaging of (a) [long MWNT]−AuNP and (b) [short MWNT]−AuNP composite materials. The white arrows guide the eye to the precise location of some adsorbed nanoparticles. Scale bars are 200 nm.

TABLE 3. Characterization of Thin and Wide MWNTs

sample	$l_{NT}/\mu m$	id_{NT}/nm	od_{NT}/nm	W_{NT}/nm	ζ/mV
thin MWNT	2.0 ± 0.3	4.4 ± 1.6	9.2 ± 2.2	10 ± 2	-11.4 ± 5.9
wide MWNT	2.0 ± 0.5	6.1 ± 1.9	29.1 ± 12.5	23 ± 7	-20.6 ± 6.5

tionship between the number of adsorbed AuNPs and MWNT surface area is evident in both systems. More importantly, the affinity toward AuNP adsorption is greater using long MWNTs than short MWNTs (prequadratic coefficients are 6.64×10^{-44} and 2.13×10^{-44} for long and short MWNTs, respectively). To support the spectroscopic observations, AuNP—MWNT composites, prepared using identical amounts of MWNTs (mass = 0.07 mg, surface area = 2.2×10^{27} nm^2), were analyzed by TEM (Figure 6).

The effect of MWNT length was clearly more subtle. Quantitative analysis, however, indicated that the density of AuNPs was higher for long MWNTs (1.4 ± 0.6 μm^{-1}, 4.8×10^{-5} nm^{-2}) than for short MWNTs (0.8 ± 0.6 μm^{-1}, 2.8×10^{-5} nm^{-2}). This corresponds to a difference of 1.8 between samples and supports the spectroscopic findings, which showed a difference of 2.0 (3.2×10^{11} NP for long MWNTs; 1.6×10^{10} NP for short MWNTs). Furthermore, the observation that longer (more polarizable) MWNTs have greater attractive interactions with nanoparticles than shorter (less polarizable) MWNTs supports previous theoretical models[31,32] and highlights the significance of van der Waals forces.

Nanotube diameter is another structural parameter that can be conveniently controlled to investigate its effect on the interactions between AuNPs and MWNTs, and two nanotube samples possessing different mean diameters (hereafter referred to as thin and wide MWNTs, respectively) were obtained by careful selection of MWNTs prepared by different methods (Table 3 and S.4 in the Supporting Information).

Microscopic analysis confirms that the mean nanotube diameter between samples is significantly different. Assuming van der Waals forces are significant, the affinity of AuNPs for wide (more polarizable) MWNTs should be greater than thin (less polarizable) MWNTs. To test this concept, comparative series of titration experiments were undertaken using AuNPs (produced by the modified citrate reduction reported by Slot and Geuze[35]) possessing inherent surface charge of -23.2 ± 4.8 mV (Figure 7).

Significantly, the affinity toward AuNP adsorption is greater using wide MWNTs than thin MWNTs (prequadratic coefficients are 9.97×10^{-43} and 1.44×10^{-44} for wide and thin MWNTs, respectively). To confirm the spectroscopic observations, AuNP—MWNT composites, prepared using identical quantities of MWNTs (mass = 0.06 mg) were analyzed by TEM (Figure 8).

Quantitative analysis indicates that the density of adsorbed AuNPs is higher for wide MWNTs (1.5 ± 0.7 μm^{-1}, 2.4×10^{-5} nm^{-2}) than for thin MWNTs (0.7 ± 0.5 μm^{-1}, 1.6×10^{-5} nm^{-2}). A quantitative comparison of the density of adsorbed AuNPs measured by TEM and UV—vis spectroscopy is less straightforward for this series of experiments, as surface area per unit nanotube mass is significantly different for wide and thin MWNTs. However, both the local-probe and the bulk characterization methods demonstrate clearly that the strength of short-range nanotube—nanoparticle interaction is higher for wider (more polarizable) MWNTs than for thinner (less polarizable) MWNTs and thus further highlight the significance of van der Waals forces.

Our measurements clearly demonstrate that the efficiency of nanotube—nanoparticle interactions is
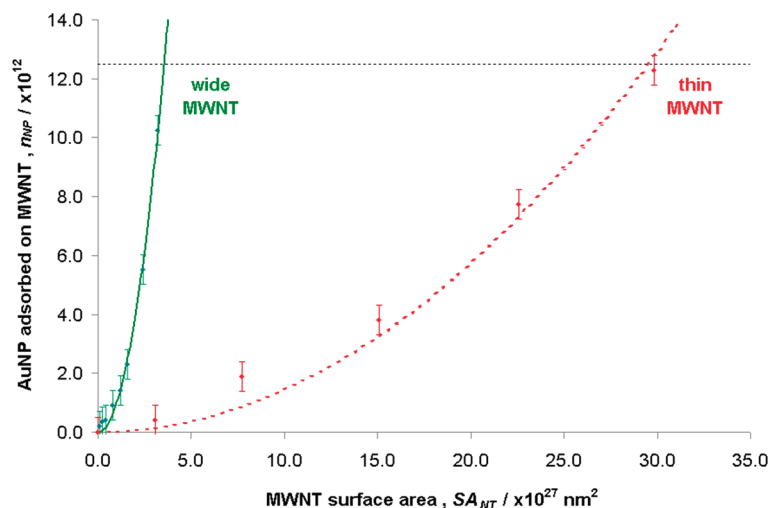

Figure 7. Adsorption isotherm correlating the number of AuNPs (n_{NP}) independently adsorbed onto wide MWNTs (green full line, $n_{NP} = 9.97 \times 10^{-43}$ $(SA_{NT})^2$, $R^2 = 0.9967$) and thin MWNT (red dashed line, $n_{NP} = 1.44 \times 10^{-44}$ $(SA_{NT})^2$, $R^2 = 0.9801$) with carbon nanotube surface area (SA_{NT}, in nm^2). The horizontal dotted line refers to the total number of nanoparticles in starting solution (1.3×10^{13}). Bars reflect the mean standard deviation from repeat measurements.
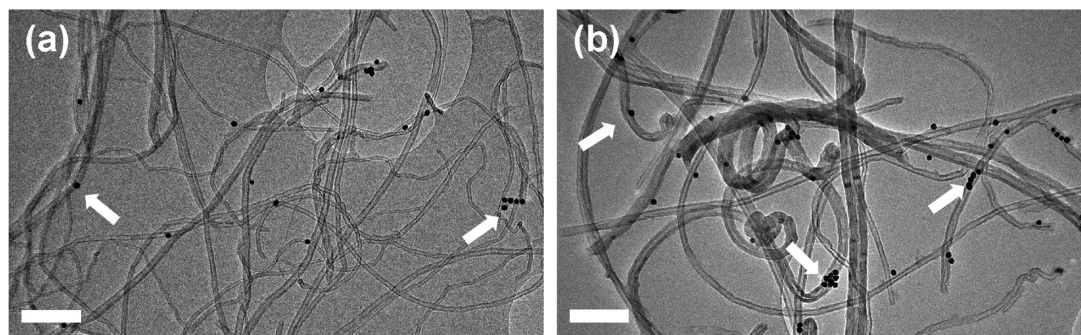
Figure 8. TEM imaging of (a) [thin MWNT]—AuNP and (b) [wide MWNT]—AuNP composite materials. The white arrows guide the eye to the precise location of some adsorbed nanoparticles. Scale bars are 200 nm.

dependent on the basic structural parameters of these materials. It is interesting that in *all* systems we studied the adsorption of AuNPs exhibits a clear quadratic dependence on the surface area of nanotubes $n_{NP} = k(SA_{NT})^2$ so that for a given system coefficient k quantitatively defines the affinity of nanoparticles for nanotubes. A logical extension of this work is to establish the relative influence of different geometric parameters for the attractive AuNP—MWNT interactions. For this purpose, we define a relative affinity factor (R_{NP}) which relates the change in the prequadratic coefficient k with respect to the change of the geometric parameter of the components:

$$R_{NP} = (k_1/k_2)/(parameter_1/parameter_2)$$

where $parameter_n$ refers to diameter/length of nanoparticle or nanotube for which the coefficient k_n was determined (Table 4). The observed relative affinity toward adsorption is not affected by nanoparticle concentration (in terms of total number of gold nanoparticles per unit volume of solution), as confirmed by a control experiment using equivalent concentrations of large and small AuNPs.

Within this framework, the nanotube diameter is the most important geometric parameter having the greatest impact on attractive interactions. The influence of nanoparticle diameter is significantly lower than that of nanotube diameter but is higher than that of nanotube length (Table 4).

CONCLUSIONS

We have investigated nanotube—nanoparticle systems where interactions are controlled by van der Waals forces. Unexpectedly, adsorption of nanoparticles on nanotubes under these conditions obeys a simple quadratic dependence on the nanotube surface area, regardless of the origin of AuNPs and MWNTs. Changes in the geometric parameters of the components have pronounced effects on the affinity of nanoparticles for nanotubes, with nanostructures of larger size exhibiting stronger attractive interactions, as a general rule. However, the impact of different parameters on van der Waals forces is not the same and decreases in the following order MWNT diameter > AuNP diameter > MWNT length. We have demonstrated that by using these simple empirical rules based on the ubiquitous van der Waals interactions the density of nanoparticles deposited on nanotubes can be precisely controlled. Since several new applications of nanotube—nanoparticle composites ranging from photovoltaics to electronic sensors to catalysis are currently being explored, an understanding of the mechanisms governing nanotube—nanoparticle interactions is timely and important. We are currently exploring the effects of variable external parameters (solvent, temperature, electromagnetic field) on the assembly of nanotube—nanoparticle heterostructures.

TABLE 4. Comparison of Relative Affinity Factors for Different Structural Parameters

	effect of MWNT diameter	effect of AuNP diameter	effect of MWNT length
R_{NP}	21.9	11.9	2.7

METHODS

Citrate-stabilized gold nanoparticles were synthesized according to established, reproducible literature techniques capable of procuring size and shape monodisperse nanocrystals.[35,38] Multiwalled carbon nanotubes were used either as-received or air-annealed.[23] Gold nanoparticle—multiwalled carbon nanotube composite materials were prepared by simple heterogeneous mixing in a suitable solvent.[20,24] In a typical experiment, a known, variable mass of dry carbon nanotube solid was added to a known, fixed volume of gold nanoparticle solution, sonicated for 30 min at room temperature, and finally purified by syringe filtration.

Supporting Information Available: Full synthetic details, light scattering, spectroscopic and microscopic confirmation of the components and afforded structures are available in the Supporting Information file. This material is available free of charge via the Internet at http://pubs.acs.org.

REFERENCES AND NOTES

1. Peng, X. H.; Chen, J. Y.; Misewich, J. A.; Wong, S. S. Carbon Nanotube−Nanocrystal Heterostructures. *Chem. Soc. Rev.* **2009**, *38*, 1076–1098.
2. Basiuk, V. A.; Basiuk, E. V. *Chemistry of Carbon Nanotubes*; American Scientific Publishers: Stevenson Ranch, CA, 2008.
3. Wildgoose, G. G.; Banks, C. E.; Compton, R. G. Metal Nanoparticles and Related Materials on Carbon Nanotubes: Methods and Applications. *Small* **2006**, *2*, 182–193.
4. Hu, X. G.; Dong, S. J. Metal Nanomaterials and Carbon Nanotubes—Synthesis, Functionalisation and Potential Applications towards Electrochemistry. *J. Mater. Chem.* **2008**, *18*, 1279–1295.
5. Eder, D. Carbon Nanotube−Inorganic Hybrids. *Chem. Rev.* **2010**, *110*, 1348–1385.
6. Daniel, M. C.; Astruc, D. Gold Nanoparticles: Assembly, Supramolecular Chemistry, Quantum Size Related Properties and Applications towards Biology, Catalysts and Nanotechnology. *Chem. Rev.* **2004**, *104*, 293–346.
7. Zhong, C. J.; Maye, M. M. Core−Shell Assembled Nanoparticles as Catalysts. *Adv. Mater.* **2001**, *13*, 1507–1511.
8. Peng, X.; Wong, S. S. Controlling Nanocrystal Density and Location on Carbon Nanotube Templates. *Chem. Mater.* **2009**, *21*, 682–694.
9. Wohltjen, H.; Snow, A. W. Size-Induced Metal to Semiconductor Transition in a Stabilized Gold Cluster Ensemble. *Chem. Mater.* **1998**, *10*, 947–949.
10. Yu, Y.; Cimeno, A.; Lan, Y. C.; Rybczynski, J.; Wang, D. Z.; Paudel, T.; Ren, Z. F.; Wagner, D. J.; Qiu, M. Q.; Chiles, T. C.; Cai, D. Assembly of Multi-functional Nanocomponents on Periodic Nanotube Arrays for Biosensors. *Micro Nano Lett.* **2009**, *4*, 27–33.
11. Jia, F.; Shan, C. S.; Li, F. H.; Niu, L. Carbon Nanotube/Gold Nanoparticle/Polyethylenimine Functionalised Ionic Liquid Thin Film Composites for Glucose Biosensing. *Biosens. Bioelectron.* **2008**, *24*, 945–950.
12. Marsh, D. H.; Rance, G. A.; Whitby, R. J.; Guistiniano, F.; Khlobystov, A. N. Assembly, Structure and Electrical Conductance of Carbon Nanotube−Gold Nanoparticle 2D Heterostructures. *J. Mater. Chem.* **2008**, *18*, 2249–2256.
13. Somani, P. R.; Somani, S. P.; Umeno, M. Application of Metal Nanoparticles Decorated Carbon Nanotubes in Photovoltaics. *Appl. Phys. Lett.* **2008**, *93*, 033315.
14. Hiemenz, P. C. *Principles of Colloid and Surface Science*; Marcel Dekker: New York, 1977.
15. Maury, P. A.; Reinhoudt, D. N.; Huskens, J. Assembly of Nanoparticles on Patterned Surfaces by Noncovalent Interactions. *Curr. Opin. Colloid Interface Sci.* **2008**, *13*, 74–80.
16. Lim, S. I.; Zhong, C. J. Molecularly Mediated Processing and Assembly of Nanoparticles: Exploring the Interparticle Interactions and Structures. *Acc. Chem. Res.* **2009**, *42*, 798–808.
17. Bishop, K. J. M.; Wilmer, C. E.; Soh, S.; Grzybowski, B. A. Nanoscale Forces and Their Uses in Self-Assembly. *Small* **2009**, *5*, 1600–1630.
18. Correa-Duarte, M. A.; Grzelczak, M.; Salgueirino-Maceira, V.; Giersig, M.; Liz-Marzan, L. M.; Farle, M.; Sierazdki, K.; Diaz, R. Alignment of Carbon Nanotubes under Low Magnetic Fields through Attachment of Magnetic Nanoparticles. *J. Phys. Chem. B* **2005**, *109*, 19060–19063.
19. Boal, A. K.; Galow, T. H.; Ilhan, F.; Rotello, V. M. Binary and Ternary Polymer-Mediated "Bricks and Mortar" Self-Assembly of Gold and Silica Nanoparticles. *Adv. Funct. Mater.* **2001**, *11*, 461–465.
20. Rance, G. A.; Khlobystov, A. N. Nanoparticle−Nanotube Electrostatic Interactions: The Effect of pH and Ionic Strength. *Phys. Chem. Chem. Phys.* **2010**, DOI: 10.1039/C001102A.
21. Suci, P. A.; Klem, M. T.; Douglas, T.; Young, M. Influence of Electrostatic Interactions on the Surface Adsorption of a Viral Protein Cage. *Langmuir* **2005**, *121*, 8686–8693.
22. Lee, S. W.; Sigmund, W. M. AFM Study of Repulsive van der Waals Forces between Teflon AF Thin Film and Silica or Alumina. *Colloids Surf., A* **2002**, *204*, 43–50.
23. Marsh, D. H.; Rance, G. A.; Zaka, M. H.; Whitby, R. J.; Khlobystov, A. N. Comparison of the Stability of Multiwalled Carbon Nanotube Dispersions in Water. *Phys. Chem. Chem. Phys.* **2007**, *9*, 5490–5496.
24. Yu, J.; Rance, G. A.; Khlobystov, A. N. Electrostatic Interactions for Directed Assembly of Nanostructured Materials: Composites of Titanium Dioxide Nanotubes with Gold Nanoparticles. *J. Mater. Chem.* **2009**, *19*, 8928–8935.
25. As the gold nanoparticle solutions employed in this study had relatively low upper threshold concentrations, varying the quantity of nanotubes and maintaining a constant volume of solvent across all experiments ensures better control over the experimental parameters.
26. Bucking, W.; Nann, T. Electrophoretic Analysis of Gold Nanoparticles: Size-Dependent Electrophoretic Mobility of Nanoparticles. *IEEE Proc.* **2006**, *153*, 47–53.
27. Sun, Y. P.; Fu, K.; Lin, Y.; Huang, W. Functionalised Carbon Nanotubes: Properties and Applications. *Acc. Chem. Res.* **2002**, *35*, 1096–1104.
28. Goodman, F. O.; Garcia, N. Roles of the Attractive and Repulsive Forces in Atomic Force Microscopy. *Phys. Rev. B* **1991**, *43*, 4728–4731.
29. Akita, S.; Nishijima, H. Nakayama, Influence of Stiffness of Carbon Nanotube Probes in Atomic Force Microscopy. *J. Phys. D* **2000**, *33*, 2673–2677.
30. Dobson, J. F.; White, A.; Rubio, A. Asymptotics of the Dispersion Interaction: Analytical Benchmarks for van der Waals Energy Functionals. *Phys. Rev. Lett.* **2006**, *96*, 073201.
31. Stolarczyk, J. K.; Sainsbury, T.; Fitzmaurice, D. Evaluation of Interactions between Functionalised Multi-Walled Carbon Nanotubes and Ligand-Stabilised Gold Nanoparticles Using Surface Element Integration. *J. Comput.-Aided Mater. Des.* **2007**, *14*, 151–165.
32. Sainsbury, T.; Stolarczyk, J.; Fitzmaurice, D. An Experimental and Theoretical Study of the Self-Assembly of Gold Nanoparticles at the Surface of Functionalised Multi-Walled Carbon Nanotubes. *J. Phys. Chem. B* **2005**, *109*, 16310–16325.
33. Kamal, C.; Ghanty, T. K.; Banerjee, A.; Chakrabarti, A. The van der Waals Coefficients between Carbon Nanostructures and Small Molecules: A Time-Dependent Density Functional Theory Study. *J. Chem. Phys.* **2009**, *131*, 167408.
34. Ma, S. J.; Guo, W. L. Size-Dependent Polarizabilities of Finite-Length Single-Walled Carbon Nanotubes. *Phys. Lett. A* **2008**, *372*, 4835–4838.
35. Slot, J. W.; Geuze, H. J. A New Method of Preparing Gold Probes for Multiple-Labelling Cyto-Chemistry. *Eur. J. Cell Biol.* **1985**, *38*, 87–93.
36. The larger radii of curvature (locally flatter nanostructures), associated with larger nanoparticles which results in greater surface contact with the nanotube, and the effect of steric interactions of surfactant molecules adsorbed on AuNPs may also contribute to the affinity of nanoparticles for nanotubes. However, the effective contribution of these factors is expected to be negligible as they are significantly more short-range as compared to relative van der Waals forces in nanotube−nanoparticle systems ($\sim 1/r^3$) and are sufficiently weak, as the organic surfactants that stabilize the nanoparticles are readily displaced upon adsorption on the nanotube surface.
37. The coverage of nanoparticles on nanotubes observed in all of the systems examined during this study is

relatively low (up to a maximum of 20 μm^{-1}) compared to other nanoparticle−nanotube composites currently documented in the literature, and this reflects the significance of electrostatic (rather than steric) factors that dictate the threshold coverage.

38. Turkevitch, J.; Stevenson, P. C.; Hillier, J. A Study of the Nucleation and Growth Processes in the Synthesis of Colloidal Gold. *Discuss. Faraday Soc.* **1951**, *11*, 55–75.